frontiers | Frontiers in Ecology and Evolution

TYPE Mini Review
PUBLISHED 10 May 2023
DOI 10.3389/fevo.2023.1199121

OPEN ACCESS

EDITED BY
Xin Jin,
Chengdu University of Technology, China

REVIEWED BY
Ana Zavattieri,
National Scientific and Technical Research Council (CONICET), Argentina
Paulo Fernandes,
University of Algarve, Portugal

*CORRESPONDENCE
Lu Jing
✉ lujing@cumtb.edu.cn

RECEIVED 03 April 2023
ACCEPTED 24 April 2023
PUBLISHED 10 May 2023

CITATION
Zhang P, Yang M, Lu J, Jiang Z, Zhou K, Xu X, Wang Y, Wu L, Chen H, Zhu X, Guo Y, Ye H, Shao L and Hilton J (2023) Floral response to the Late Triassic Carnian Pluvial Episode. *Front. Ecol. Evol.* 11:1199121. doi: 10.3389/fevo.2023.1199121

Floral response to the Late Triassic Carnian Pluvial Episode

Peixin Zhang[1,2], Minfang Yang[3], Jing Lu[2]*, Zhongfeng Jiang[1], Kai Zhou[4], Xiaotao Xu[5], Ye Wang[2], Li Wu[1], Huijuan Chen[1], Xuran Zhu[1], Yanghang Guo[1], Huajun Ye[1], Longyi Shao[2] and Jason Hilton[6]

[1]School of Municipal and Environmental Engineering, Henan University of Urban Construction, Pingdingshan, Henan, China, [2]State Key Laboratory of Coal Resources and Safe Mining, College of Geoscience and Surveying Engineering, China University of Mining and Technology, Beijing, China, [3]Research Institute of Petroleum Exploration and Development, PetroChina, Beijing, China, [4]State Key Laboratory of Hydroscience and Engineering, Department of Hydraulic Engineering, Tsinghua University, Beijing, China, [5]General Prospecting Institute of China National Administration of Coal Geology, Beijing, China, [6]School of Geography, Earth and Environmental Sciences, The University of Birmingham, Birmingham, United Kingdom

The Late Triassic Carnian Pluvial Episode (CPE; *ca.* 234–232 Ma) was characterized by dramatic global temperature and humidity increases, which in many terrestrial settings was accompanied by changes from arid to humid vegetation types. This study reviews current evidence of terrestrial floral composition and distribution during the CPE and analyzes spatial and temporal variation with relation to potential environmental driving mechanisms. Available evidence suggests the CPE was a globally significant event that triggered significant increases in the abundance of ferns and hygrophytes in terrestrial floras and freshwater algae in fluvial and lacustrine settings. These changes ended a long interval of relatively arid terrestrial climatic conditions since the Early Triassic and are linked temporally with eruptions of the oceanic plateau Wrangellia Large Igneous Province (LIP). The massive release of greenhouse gasses including isotopically light CO_2 during 3–4 distinct pulses of Wrangellia volcanism appears to have been the main driver of CPE climate change. Each pulse enhanced global atmospheric circulation and the hydrological cycle and resulted in changes from arid to humid conditions that affected floral abundance and composition. Higher terrestrial primary productivity in humid phases facilitated increased burial of terrestrial organic carbon and led to the recommencement of peat accumulation, ending the coal gap that had persisted since the earliest Triassic times. Enhanced movement of carbon from the atmosphere through the biosphere into the geosphere may have counteracted the warming effects of Wrangellia volcanic greenhouse gas emissions and ultimately led to the return of a steady climate state that terminated the warm and humid conditions of the CPE.

KEYWORDS

Late Triassic, Wrangellia LIP, floral change, hygrophytes, volcanic induced climate change

1. Introduction

The Carnian Pluvial Episode (*ca.* 234 to 232 Ma; CPE) was a significant global environmental and climatic event during the Carnian Stage of the Late Triassic (Simms and Ruffell, 1989; Sun et al., 2016; Dal Corso et al., 2020; Lu et al., 2021). It is considered an important turning point in the long-term recovery of the ecosystem and organism diversity after the global-scale devastation of the

Permian–Triassic mass extinction (PTME) and its extended aftermath (Dal Corso et al., 2020, 2022a) and has been hailed as a dawn of modern ecosystems (Dal Corso et al., 2020). The CPE is characterized by dramatic climatic warming, increased global rainfall, and relatively humid climatic conditions (e.g., Dal Corso et al., 2020) and is accompanied by significant fluctuations in the carbon cycle (Sun et al., 2016; Miller et al., 2017; Dal Corso et al., 2018, 2020; Shi et al., 2019; Lu et al., 2021; Li Q. et al., 2022), the shutdown of carbonate platform productivity (Shi et al., 2017), eustatic sea-level fall and modifications in carbonate platforms (Jin et al., 2020, 2022a), widespread anoxia in oceans and lakes (Sun et al., 2016; Dal Corso et al., 2020; Lu et al., 2021), elevated extinction rates (especially in ammonoids, conodonts and crinoids) (Simms and Ruffell, 1989; Bernardi et al., 2018; Dal Corso et al., 2020), and increased biodiversity including the origination of major groups of modern conifers, dinosaurs, and calcium nanobiotes (Simms and Ruffell, 1989; Bernardi et al., 2018; Dal Corso et al., 2020). The temporal coincidence of the CPE and the Wrangellia Large Igneous Province (LIP) suggests a causal relationship through release of large amounts of CO_2 into the atmosphere-marine system, resulting in an enhancement of the global atmospheric circulation and hydrological cycle (Dal Corso et al., 2020; Lu et al., 2021; Mazaheri-Johari et al., 2021; Zhao et al., 2022; Jin et al., 2023).

Enhanced atmospheric circulation and hydrological cycles have been considered potential drivers for major changes in global floras during the CPE (Dal Corso et al., 2020; Lu et al., 2021). In the Gondwana supercontinent, previous studies have shown that the terrestrial macroflora is dominated by corystosperm seed ferns (pteridosperms), and spore and pollen fossils (Kustatscher et al., 2018). In Laurasia, a transition from arid to humid floras occurred during the Carnian stage and was accompanied by thick coal seams (Pott et al., 2008). These coals mark the re-commencement of peat accumulation after the global coal gap (Retallack et al., 1996) that followed the collapse of Permian–Triassic terrestrial ecosystems (Retallack et al., 1996; Dal Corso et al., 2020, 2022a,b; Zhang et al., 2023a; Figure 1). Palynological studies have independently identified increases in hygrophytic plant abundance through the CPE in the boreal realm (Mueller et al., 2016a), the northeastern Tethys region (Mazaheri-Johari et al., 2022), the western Tethys region (Roghi, 2004; Roghi et al., 2010; Mueller et al., 2016b; Baranyi et al., 2019b; Fijałkowska-Mader et al., 2021), and the eastern Tethys region (Lu et al., 2021; Li L. et al., 2022; Peng et al., 2022), collectively indicating that a relatively humid climate prevailed (Figure 1). However, palynological studies from the Denmark Basin (Lindström et al., 2017) and the United Kingdom (Baranyi et al., 2019a) did not show significant floral changes or increased humid climatic conditions during the CPE, showing that the climatic effects varied spatially. Thus, the global extent of the effects of CPE and the relatively humid climatic conditions that prevailed during this period remains somewhat controversial.

In this study, we review the current evidence for terrestrial floral changes during the CPE and evaluate the information on climatic and environmental change this provides. We also investigate the relationship between floral changes and massive volcanism during the CPE.

2. Age constraints and duration of the CPE

Based on the available evidence from biostratigraphy (including fossil ammonoids, conodonts, and palynomorphs) and carbon isotope chemostratigraphy, markers for the commencement of the CPE are recognized in marine, marine-continental transitional, and continental strata (Dal Corso et al., 2020; Lu et al., 2021; Li Q. et al., 2022; Figures 1, 2). The onset of the CPE coincided with the first appearance of the ammonoid genus *Austrotrachyceras* in the Julian substage of the Carnian (Simms and Ruffell, 1989; Dal Corso et al., 2012, 2015; Sun et al., 2016) and was accompanied by a negative carbon isotope excursion (CIE-I) (Dal Corso et al., 2018, 2020) and an increase in the proportion of terrestrial hygrophyte plants (Mueller et al., 2016b; Lu et al., 2021; Figures 2, 3). Correlation between biostratigraphic data and the high-resolution C-isotope patterns suggests that ~3–4 separate CIEs punctuated the CPE interval (Miller et al., 2017; Dal Corso et al., 2018; Lu et al., 2021; Tomimatsu et al., 2021; Li Q. et al., 2022; Figure 2). In contrast, the timing of the end of the CPE is less well constrained, with current evidence placing this at the base or within the Tuvalian 2 substage of the Carnian, based on sedimentological (end of terrigenous sediment supply) and chemostratigraphic (CIE-IV) evidence (Dal Corso et al., 2020; Lu et al., 2021; Figure 2).

Based on cyclostratigraphy, biostratigraphy, magnetostratigraphy, chemostratigraphy, and zircon U–Pb dating, previous studies have determined that the CPE occurred between *ca.* 234 and 232 Ma and lasted ~1.09 to 1.7 Ma from the late Julian 1 to the Tuvalian 2 substages of the Carnian (Zhang et al., 2015; Miller et al., 2017; Bernardi et al., 2018; Lu et al., 2021). In South China, the CPE has been constrained by sedimentology (transition from carbonate-rich to clastic-rich facies), magnetostratigraphy (an interval of reversed polarity), and cyclostratigraphy (405 kyr long-eccentricity cycle from spectral gamma-ray intensity curve) from which the CPE is estimated to have approximately lasted 1.3 Ma (Zhang et al., 2015). In the United Kingdom, the CPE has been constrained by chemostratigraphy (four CIEs) and cyclostratigraphy (405 kyr long-eccentricity of Ca/Ti elements) and is interpreted to have lasted ~1.09 Ma (Miller et al., 2017). In the Dolomites (Italy), the duration of the CPE has been constrained by sedimentology (significant pulse of humid climatic conditions inferred from four sudden increases in terrigenous material entering the basin interior), chemostratigraphy (four CIEs), and biostratigraphy (restriction by *Aonoides*/*Austriacum* and *Subbullatus*), showing that the CPE may have lasted 1.6 to 1.7 Ma (Bernardi et al., 2018; Dal Corso et al., 2018). In North China, CPE has been constrained by biostratigraphy (increased hygrophyte plants), chemostratigraphy (four CIEs), two zircon U–Pb dates, and calculations made from deposition rates calibrated by zircon U–Pb dates, that show the CPE may have lasted ~1.6 Ma (Lu et al., 2021).

3. CPE-related floral and climatic changes

Previous studies have shown that the enhancement of atmospheric circulation and hydrological cycles during the CPE resulted in significant changes in the terrestrial flora from xerophyte to hygrophyte-dominated (Dal Corso et al., 2020; Lu et al., 2021; Figure 3). During the CPE, climatic changes also facilitated the radiation and diversification of plant groups including gymnosperms (Bennettitales and conifers) and ferns (Hymenophyllaceae, Matoniaceae and Dipteridaceae) (Figure 3). Each of these groups subsequently became major components in Mesozoic and, in some

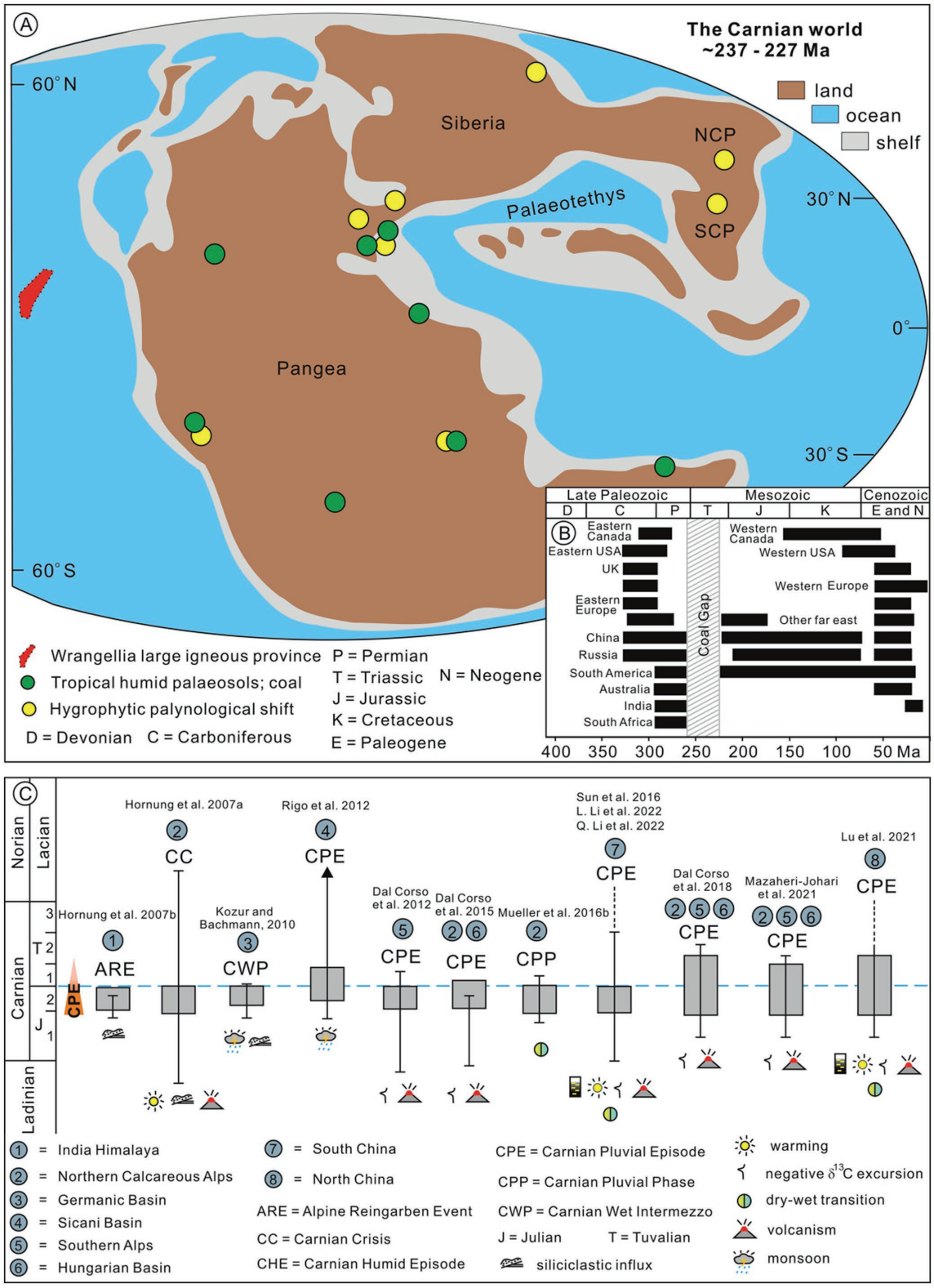

FIGURE 1
Environmental and geochemical changes during the Carnian Pluvial Episode (CPE). **(A)** Palaeogeography during the Carnian and location of the data indicating environmental changes during the CPE (modified from Dal Corso et al., 2020). **(B)** Long-term changes in coal distribution showing the "Coal Gap" from the Late Permian to Middle Triassic (modified from Retallack et al., 1996). **(C)** Summary of previous studies on the CPE. Gray shading represents the short-lived CPE interval (data are form Hornung et al., 2007a,b; Kozur and Bachmann, 2010; Dal Corso et al., 2012; Rigo et al., 2012; Dal Corso et al., 2015; Sun et al., 2016; Mueller et al., 2016b; Dal Corso et al., 2018; Shi et al., 2019; Lu et al., 2021; Mazaheri-Johari et al., 2021; Li L. et al., 2022).

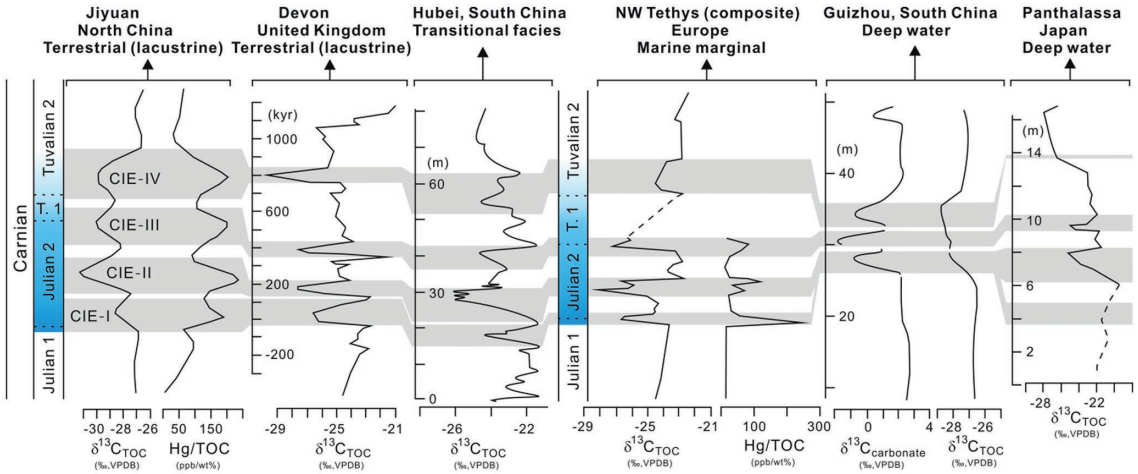

FIGURE 2
Reference C-isotope and Hg records across the Carnian Pluvial Episode (CPE). Data are from North China (Lu et al., 2021); the United Kingdom (Miller et al., 2017); Hubei, South China (Li Q. et al., 2022); Guizhou, South China (Sun et al., 2016); Northwestern Tethys (Dal Corso et al., 2018; Mazaheri-Johari et al., 2021); and Japan (Tomimatsu et al., 2021). T. 1=Tuvalian 1; CIE-I to CIE-IV=organic carbon isotope excursion I to IV.

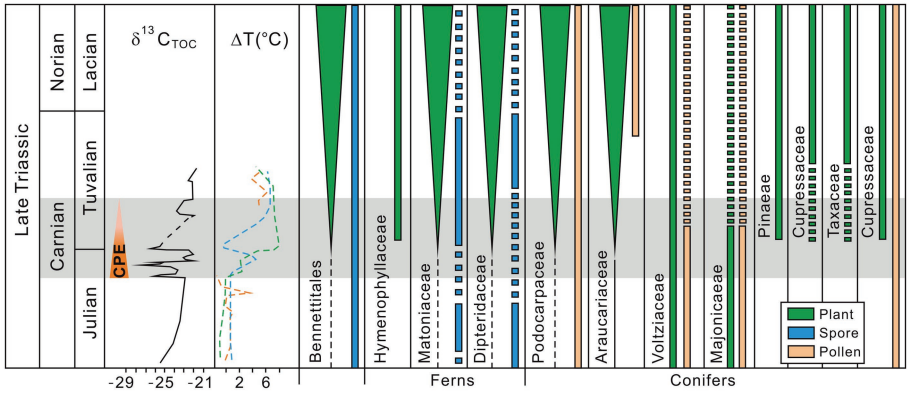

FIGURE 3
Major floristic changes in relation to C-isotope and temperature variations recorded during the Carnian period. C-isotope data from Dal Corso et al. (2018); O-isotope data from Hornung et al. (2007a), Trotter et al. (2015), and Sun et al. (2016); floral data from Roghi (2004), Mueller et al. (2016a,b), Kustatscher et al. (2018), Baranyi et al. (2019a,b), Dal Corso et al. (2020 and references therein), Lu et al. (2021), Li Q. et al., (2022), and Peng et al. (2022).

cases, modern floras (Dal Corso et al., 2020 and references therein) (Figure 3).

The Late Triassic plant macrofossil record is sporadic and generally only recognizable at the stage level, making it difficult to accurately track floral changes through the CPE interval (from Julian to late Tuvalian substages) (Dal Corso et al., 2020). However, there is an overall transition from xerophytes to hygrophytes in the flora of the Carnian stage (Roghi, 2004; Roghi et al., 2010; Baranyi et al., 2019b; Figure 3). In South China, sphenophytes, ferns, seed ferns, and cycads/bennettitaleans are common in the Carnian Daqiaodi flora in Sichuan-Yunnan provinces and the Jiuligang flora in Hubei province (Zhou and Zhou, 1983). In Europe, the Lunz flora is representative of the Carnian macroflora and is dominated by an abundance of ferns and cycads/bennettitaleans, with sphenophytes common and ginkgophytes and conifers less abundant (Pott et al., 2008; Mueller et al., 2016b; Kustatscher et al., 2018). In North China, xerophytic floras dominated by the conifer *Voltzia* were widespread in the Middle Triassic Ermaying Formation (Liu et al., 2018). However, the Late Triassic Yanchang Formation flora (Sun et al., 2020) lacked these xerophytic elements and reflected more humid conditions. Using U–Pb dating and the change to more humid floras allows the CPE to be placed in the Yangchang Formation (Sun et al., 2020).

Plant macrofossils are strongly susceptible to taphonomic bias affecting their distribution and preservation potential in different sedimentary environments (e.g., DiMichele et al., 2020), so caution must be applied to literal readings of the plant macrofossil record. In contrast, habitat heterogeneity affects palynological spores and pollen fossils less, as they can be readily transported by wind and water and tend to have better taphonomic preservation potential than plant macrofossils (e.g., Marchetti et al., 2022). Spore and pollen fossils

more accurately reflect broad patterns of floral change than plant macrofossils during the CPE. Palynological studies of the Western Tethys region have shown significant changes in plant types and climatic conditions during the CPE. In northeastern Italy, an increase in abundance of lycopod and fern spores from the late Julian to early Tuvalian substages indicates that relatively humid climatic conditions prevailed (Roghi, 2004). In northern Norway, elevated spore abundances (including *Concavisporites* and *Deltoidispora*) and coal seams occur in the De Geerdalen Formation, suggesting that relatively warm and humid climate conditions prevailed during the late Julian substage (Hounslow et al., 2007; Mueller et al., 2016a). In Austria, increases in hygrophyte sporomorphs (including all spores and *Cycadopites*, *Alisporites*, and *Aulisporites* pollen) and the hygrophyte/xerophyte (H/X) ratio were recorded in the Julian 2 substage, indicating relatively humid climatic conditions and widespread intensification of the hydrological cycle (Roghi et al., 2010; Mueller et al., 2016b; Figure 4). In Western Hungary, an increase in hygrophyte sporomorphs (including all spores identified and *Cycadopites* and *Aulisporites* pollen) and elevated H/X ratio accompanies high kaolinite concentrations in the Julian 2 substage (Dal Corso et al., 2018; Baranyi et al., 2019b). Kaolinite forms in terrestrial settings as a weathering product of felsic minerals under humid conditions (e.g., Zhang et al., 2022a), thus indicating relatively humid climatic conditions and intensive terrestrial runoff (Dal Corso et al., 2018; Baranyi et al., 2019b; Figure 4). In Poland, a marked shift occurs from xerophyte (including all spores and *Aulisporites* pollen) to hygrophyte (including all other pollen except *Cycadopites* and *Monosulcites*) dominated flora during the CPE, accompanied by paleosol changes from aridisols to poorly drained hydric soils, suggest relatively humid climatic conditions prevailed (Fijałkowska-Mader et al., 2021). In the Aghdarband Basin of northeast Iran, the dominance of hygrophytic plant spores and coal seams in the lowest part of the Miankuhi Formation suggest that relatively humid climatic conditions prevailed during the Julian 2 substage (Mazaheri-Johari et al., 2022).

Palynological studies of the Eastern Tethys region also have shown significant changes in plant types and climatic conditions during the CPE. In North China, high abundance of fern spores (including *Cyclogranisporites*, *Osmundacidites*, and *Punctatisporites*) and freshwater algae, as well as increases in hygrophyte sporomorphs (including all spores identified and *Cycadopites*, *Alisporites*, and *Aulisporites* pollen) and the H/X ratio, show significant increases from the Julian 2 to early Tuvalian substages and indicate humid climatic conditions (Lu et al., 2021; Figure 4). In South China, an abundance of ferns (especially Dipteridaceae/Matoniaceae) and an increase in the hygrophyte group (including ferns, horsetails, lycopsids, mosses, and seed ferns) and H/X ratio in the Ma'antang Formation during the Julian 2 substage also indicates relatively humid climatic conditions (Li L. et al., 2022; Figure 4). In the Junggar Basin of northwest China, the Huangshanjie Formation recorded a shift from a conifer-dominated forest community (with common ginkgophytes and bennettites) to a fern-dominated community, showing a change from arid to relatively humid climatic conditions during the CPE (Peng et al., 2022).

In summary, most palynological studies from Western and Eastern Tethys regions show an increase in the abundance of hygrophyte plants and an increase in the H/X ratio during the CPE, suggesting relatively humid climatic conditions were globally widespread at that time. This agrees with the sedimentary evidence from the Central European Basin (Simms and Ruffell, 1989), the Newark Basin (North America; Olsen, 1997), Morocco (Mader et al., 2017), East Greenland (Andrews and Decou, 2019), the Wessex Basin (United Kingdom; Baranyi et al., 2019a), the Ischigualasto Basin (Argentina; Mancuso et al., 2020), and the Jiyuan Basin (North China;

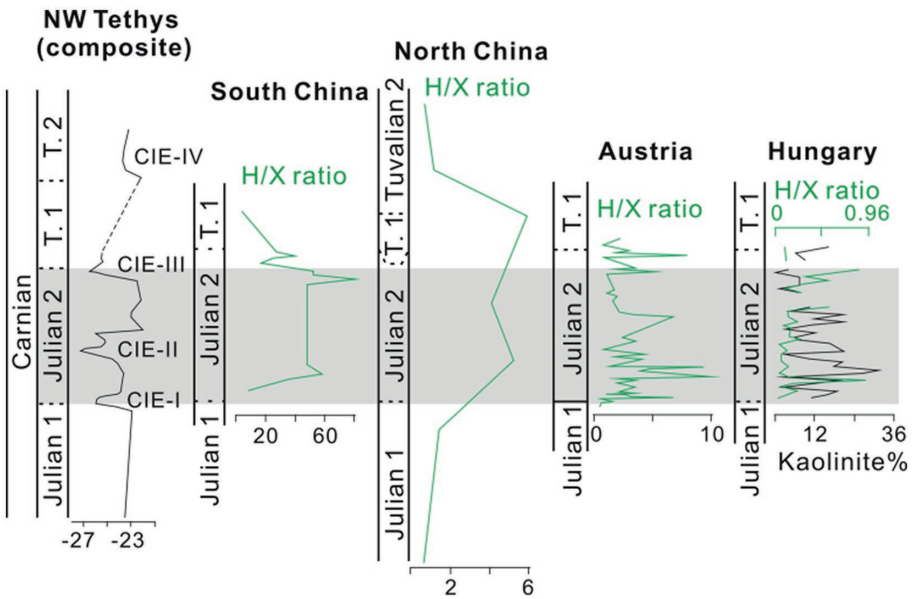

FIGURE 4
Correlation of C-isotope records and the hygrophyte/xerophyte (H/X) ratio between eastern and western Tethys regions during the Carnian Pluvial Episode (CPE). C-isotope data from Dal Corso et al. (2018); H/X ratio data are from South China (Li L. et al., 2022), North China (Lu et al., 2021), Austria (Mueller et al., 2016b), and Hungary (Baranyi et al., 2019b).

Lu et al., 2021) that show increases in terrestrial runoff, lake deepening and/or area expansion, and prevailing relatively humid climatic conditions during the CPE. Therefore, we consider that the significant changes in terrestrial floras during the CPE represent a global humid event.

4. Causal link with Wrangellia volcanism

In recent years LIP eruptions have increasingly been identified as major drivers for changes in terrestrial environments and floras globally at different stratigraphic times (Dal Corso et al., 2020; Lu et al., 2020, 2021; Shen et al., 2022; Jin et al., 2022b, 2023; Zhang et al., 2022b, 2023a,b). As outlined above (see Section 3), studies of widely distributed plant macro- and microfossils have revealed significant synchronous changes in terrestrial flora during the CPE. Time-dependent coupling relationship among these changes and Hg concentration anomalies and Carbon Isotope Excursions (CIEs) in sedimentary successions and global warming (Figures 2, 3) identifies the Wrangellia LIP as a likely driver for climate changes during the CPE (Dal Corso et al., 2018, 2020; Lu et al., 2021; Mazaheri-Johari et al., 2021; Zhao et al., 2022; Jin et al., 2023).

Sedimentary Hg records serve as proxies for volcanism in deep time and reveal that there were 3–4 pulses of volcanism during the CPE interval (Dal Corso et al., 2020; Lu et al., 2021; Mazaheri-Johari et al., 2021; Zhao et al., 2022; Jin et al., 2023). Each eruption released large amounts of isotopically light CO_2 into the reservoir of the exogenic carbon cycle, which led to global warming and a significant carbon cycle fluctuation (Dal Corso et al., 2020; Lu et al., 2021; Figure 5). As observed in other regions including Western Tethys, South China, North China, and Japan, the close correspondence between Hg concentrations (or Hg/TOC peaks) and CIEs during the CPE interval indicates the entry of large amounts of isotopically light carbon into the atmosphere–ocean system directly from volcanism (Lu et al., 2021; Mazaheri-Johari et al., 2021; Zhao et al., 2022; Jin et al., 2023; Figure 2). Similarly, multiple CIEs and oxygen isotope variations from the western and eastern Tethys (Hornung et al., 2007a; Trotter et al., 2015; Sun et al., 2016; Dal Corso et al., 2020), as well as results from biogeochemical box models based on the CIEs and Hg/TOC ratios (Dal Corso et al., 2022b), provide evidence for global carbon cycle fluctuations and warming climatic conditions during the CPE. Higher temperatures promoted the evaporation of water vapor, thus increasing the water saturation in the atmosphere and the temperature differences between the oceans and the land, leading to the intensification of atmospheric circulation and hydrological cycle (Figure 5). Increased hydrological cycle and atmospheric circulation led to increased terrestrial precipitation, that in turn may have culminated in a significant shift from arid to humid climatic conditions (see Section 3).

During the CPE, changes in terrestrial climatic conditions from arid and semi-arid to humid were favorable to plant growth and would have increased terrestrial primary productivity. Increased primary productivity promoted global peat accumulation and significantly increased organic carbon amount and burial rate in the geosphere (e.g., Retallack et al., 1996; Dal Corso et al., 2020, 2022b; Lu et al., 2021). Such a change would have been critical to recommencing thick peat accumulation worldwide after the coal-gap (Figures 1, 5). Furthermore, each of the separate pulses of CPE volcanism resulted in the same general pattern, including increases in temperature and humidity, changes in floral composition with an increase in the proportion of hygrophytic plants, and also increases in primary organic productivity (Dal Corso et al., 2020; Lu et al., 2021). Increases in humidity resulted in elevating lake levels and changing large parts of sedimentary basin interiors into swamps (Dal Corso et al., 2020; Lu et al., 2021). The humid climate conditions in the CPE also promoted enhanced continental chemical weathering rates (e.g., Baranyi et al., 2019b; Pecorari et al., 2023), which led to increased nutrients yields in fluvial, swamp, and lacustrine environments. Increased nutrient levels in terrestrial watercourses, in turn, led to increased primary organic productivity and blooms of freshwater algae and eutrophication, as evidenced by the increased abundance of freshwater algae in North China and the UK (Baranyi et al., 2019a; Lu et al., 2021), and a decrease in the Carbon/Nitrogen (C/N) ratio in North China reflecting a shift from terrestrial (C-rich) to fluvial/lacustrine (N-rich) sources of organic matter in lakes (Lu et al., 2021). The increase in plant and freshwater algae primary productivity would have increased the draw-down of additional atmospheric CO_2 through plant photosynthesis and most likely played an essential role in controlling the atmospheric composition by counteracting the warming effects of greenhouse gas emissions. This may have helped drive climatic conditions toward a steady state after pulses of volcanism subsided, which may have ended the CPE once Wrangellian volcanism ceased (Figure 5).

5. Conclusion

Studies of plant macro- and microfossils widely distributed around the Tethys suggest a global nature of the environmental and floral effects of the CPE. During the CPE, significant increases in the abundance of terrestrial hygrophytes (including ferns) and freshwater algae and increased H/X ratios indicate that relatively warm and humid climatic conditions prevailed. These are best explained by an intensification of global atmospheric circulation and the hydrological cycle caused by the release of large amounts of greenhouse gases from the Wrangellia LIP. Changes in climatic conditions from arid to humid enabled increased terrestrial primary productivity and an increased proportion of hygrophytic plants and also led to changes in sedimentary environments, including rising lake water levels, lake area expansion, and forming extensive swamps in continental basin interiors. Collectively these changes promoted the reoccurrence of global peat accumulation after the "coal gap" and led to increased organic carbon abundance and burial in terrestrial sediments. Increased terrestrial primary productivity and burial would have helped offset global warming caused by greenhouse gas emissions from volcanism through a more significant draw-down of CO_2 by photosynthesis. Increased draw-down of CO_2 through the CPE

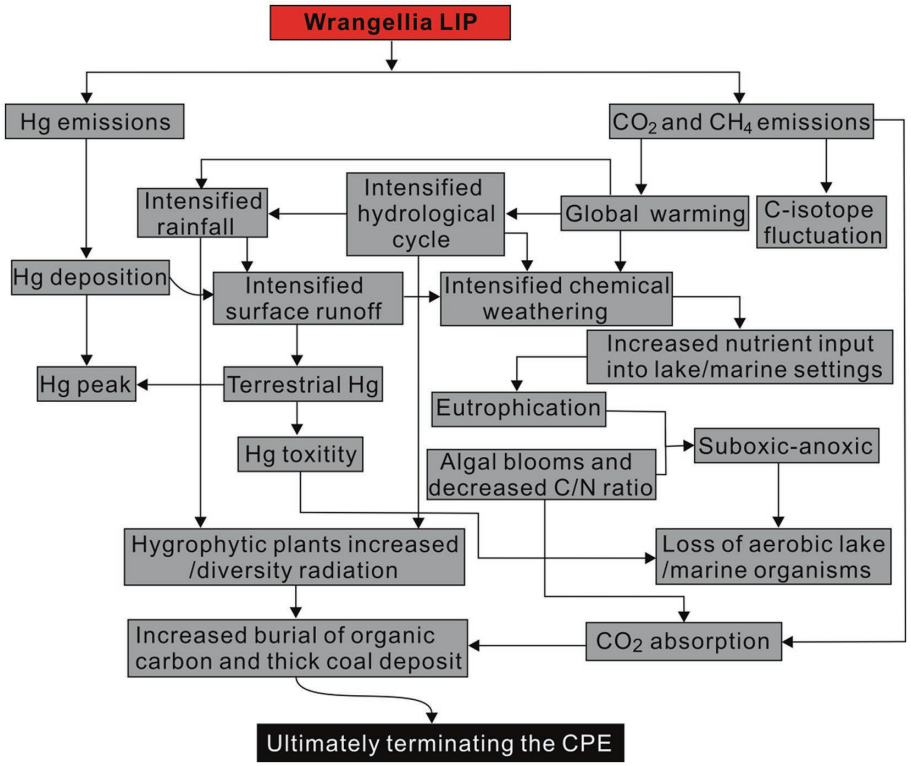

FIGURE 5
Flow chart illustrating cause-and-effect relationships among the Wrangellia LIP and the changes in terrestrial environments, climates, and flora.

likely played an important role in returning post-volcanism climates to steady states ultimately leading the end of the CPE post-volcanism.

Author contributions

PZ, MY, JL, LS, and JH designed the research. JL, PZ, MY, LS, and JH wrote the paper. All authors contributed to the article and approved the submitted version.

Funding

Financial support was provided by the National Key Research and Development Program of China (2021YFC2902000), the Open Fund of National Energy Shale Gas Research and Development Centre (2022-KFKT-14), the Fund of Henan University of Urban Construction (K-Q2023019), the National Natural Science Foundation of China (Grant nos. 42172196, 41772161, and 41472131), and the National Science and Technology Major Project (Award no. 2017ZX05009-002).

Acknowledgments

We thank Xin Jin, Paulo Fernandes, and Ana Zavattieri for constructive and helpful reviews of the manuscript.

Conflict of interest

MY was employed by PetroChina.

The remaining authors declare that the research was conducted in the absence of any commercial or financial relationships that could be construed as a potential conflict of interest.

Publisher's note

References

Andrews, S. D., and Decou, A. (2019). The Triassic of Traill Ø and Geographical Society Ø, East Greenland: implications for North Atlantic palaeogeography. *Geol. J.* 54, 2124–2144. doi: 10.1002/gj.3287

Baranyi, V., Miller, C. S., Ruffell, A., Hounslow, M. W., and Kürschner, W. M. (2019a). A continental record of the carnian pluvial episode (CPE) from the Mercia mudstone group (UK): palynology and climatic implications. *J. Geol. Soc. Lond.* 176, 149–166. doi: 10.1144/jgs2017-150

Baranyi, V., Rostási, Á., Raucsik, B., and Kürschner, W. M. (2019b). Palynology and weathering proxies reveal climatic fluctuations during the Carnian Pluvial Episode (CPE) (Late Triassic) from marine successions in the Transdanubian Range

(western Hungary). *Glob. Planet. Change* 177, 157–172. doi: 10.1016/j.gloplacha.2019.01.018

Bernardi, M., Gianolla, P., Petti, F. M., Mietto, P., and Benton, M. J. (2018). Dinosaur diversification linked with the Carnian Pluvial Episode. *Nat. Commun.* 9:1499. doi: 10.1038/s41467-018-03996-1

Dal Corso, J., Bernardi, M., Sun, Y., Song, H., Seyfullah, L. J., Preto, N., et al. (2020). Extinction and dawn of the modern world in the Carnian (Late Triassic). *Sci. Adv.* 6:eaba0099. doi: 10.1126/sciadv.aba0099

Dal Corso, J., Gianolla, P., Newton, R. J., Franceschi, M., Roghi, G., Caggiati, M., et al. (2015). Carbon isotope records reveal synchronicity between carbon cycle perturbation and the "Carnian Pluvial Event" in the Tethys realm (Late Triassic). *Glob. Planet. Change* 127, 79–90. doi: 10.1016/j.gloplacha.2015.01.013

Dal Corso, J., Gianolla, P., Rigo, M., Franceschi, M., Roghi, G., Mietto, P., et al. (2018). Multiple negative carbon-isotope excursions during the Carnian Pluvial Episode (Late Triassic). *Earth-Science Rev.* 185, 732–750. doi: 10.1016/j.earscirev.2018.07.004

Dal Corso, J., Mietto, P., Newton, R. J., Pancost, R. D., Preto, N., Roghi, G., et al. (2012). Discovery of a major negative ^{13}C spike in the Carnian (Late Triassic) linked to the eruption of Wrangellia flood basalts. *Geology* 40, 79–82. doi: 10.1130/G32473.1

Dal Corso, J., Mills, B. J. W., Chu, D., Newton, R. J., and Song, H. (2022a). Background Earth system state amplified Carnian (Late Triassic) environmental changes. *Earth Planet. Sci. Lett.* 578:117321. doi: 10.1016/j.epsl.2021.117321

Dal Corso, J., Song, H., Callegaro, S., Chu, D., Sun, Y., Hilton, J., et al. (2022b). Environmental crises at the Permian–Triassic mass extinction. *Nat. Rev. Earth Environ.* 3, 197–214. doi: 10.1038/s43017-021-00259-4

DiMichele, W. A., Bashforth, A. R., Falcon-Lang, H. J., and Lucas, S. G. (2020). Uplands, lowlands, and climate: Taphonomic megabiases and the apparent rise of a xeromorphic, drought-tolerant flora during the Pennsylvanian-Permian transition. *Palaeogeogr. Palaeoclimatol. Palaeoecol.* 559:109965. doi: 10.1016/j.palaeo.2020.109965

Fijałkowska-Mader, A., Jewuła, K., and Bodor, E. (2021). Record of the Carnian Pluvial Episode in the Polish microflora. *Palaeoworld* 30, 106–125. doi: 10.1016/j.palwor.2020.03.006

Hornung, T., Brandner, R., Krystyn, L., Joachimski, M. M., and Keim, L. (2007a). Multistratigraphic constraints on the NW Tethyan Carnian crisis. *New Mex. Museum Nat. Hist. Sci. Bull.* 41, 59–67.

Hornung, T., Krystyn, L., and Brandner, R. (2007b). A Tethys-wide mid-Carnian (Upper Triassic) carbonate productivity crisis: evidence for the Alpine Reingraben Event from Spiti (Indian Himalaya)? *J. Asian Earth Sci.* 30, 285–302. doi: 10.1016/j.jseaes.2006.10.001

Hounslow, M. W., Hu, M., Mørk, A., Vigran, J. O., Weitschat, W., and Orchard, M. J. (2007). Magneto-biostratigraphy of the Middle to Upper Triassic transition, Central Spitsbergen, arctic Norway. *J. Geol. Soc. Lond.* 164, 581–597. doi: 10.1144/0016-76492005-184

Jin, X., Franceschi, M., Martini, R., Shi, Z., Gianolla, P., Rigo, M., et al. (2022a). Eustatic sea-level fall and global fluctuations in carbonate production during the Carnian Pluvial Episode. *Earth Planet. Sci. Lett.* 594:117698. doi: 10.1016/j.epsl.2022.117698

Jin, X., Gianolla, P., Shi, Z., Franceschi, M., Caggiati, M., Du, Y., et al. (2020). Synchronized changes in shallow water carbonate production during the Carnian Pluvial Episode (Late Triassic) throughout Tethys. *Glob. Planet. Change* 184:103035. doi: 10.1016/j.gloplacha.2019.103035

Jin, X., Tomimatsu, Y., Yin, R., Onoue, T., Franceschi, M., Grasby, S. E., et al. (2023). Climax in Wrangellia LIP activity coincident with major Middle Carnian (Late Triassic) climate and biotic changes: mercury isotope evidence from the Panthalassa pelagic domain. *Earth Planet. Sci. Lett.* 607:118075. doi: 10.1016/j.epsl.2023.118075

Jin, X., Zhang, F., Baranyi, V., Kemp, D. B., Feng, X., Grasby, S. E., et al. (2022b). Early Jurassic massive release of terrestrial mercury linked to floral crisis. *Earth Planet. Sci. Lett.* 598:117842. doi: 10.1016/j.epsl.2022.117842

Kozur, H. W., and Bachmann, G. H. (2010). The Middle Carnian wet intermezzo of the Stuttgart formation (Schilfsandstein), Germanic Basin. *Palaeogeogr. Palaeoclimatol. Palaeoecol.* 290, 107–119. doi: 10.1016/j.palaeo.2009.11.004

Kustatscher, E., Ash, S. R., Karasev, E., Pott, C., Vajda, V., Yu, J., et al. (2018). Flora of the Late Triassic. *Late Triassic World* 46, 545–622. doi: 10.1007/978-3-319-68009-5_13

Li, L., Kürschner, W. M., Lu, N., Chen, H., An, P., and Wang, Y. (2022). Palynological record of the Carnian Pluvial Episode from the northwestern Sichuan Basin, SW China. *Rev. Palaeobot. Palynol.* 304:104704. doi: 10.1016/j.revpalbo.2022.104704

Li, Q., Ruhl, M., Wang, Y. D., Xie, X. P., An, P. C., and Xu, Y. Y. (2022). Response of Carnian Pluvial Episode evidenced by organic carbon isotopic excursions from western Hubei, South China. *Palaeoworld* 31, 324–333. doi: 10.1016/j.palwor.2021.08.004

Lindström, S., Erlström, M., Piasecki, S., Nielsen, L. H., and Mathiesen, A. (2017). Palynology and terrestrial ecosystem change of the Middle Triassic to lowermost Jurassic succession of the eastern Danish Basin. *Rev. Palaeobot. Palynol.* 244, 65–95. doi: 10.1016/j.revpalbo.2017.04.007

Liu, J., Ramezani, J., Li, L., Shang, Q., Xu, G. H., Wang, Y. Y., et al. (2018). High-precision temporal calibration of middle Triassic vertebrate biostratigraphy: U-Pb zircon constraints for the Sinokannemeyeria Fauna and Yonghesuchus. *Vertebr. Palasiat.* 56, 16–24. doi: 10.19615/j.cnki.1000-3118.170808

Lu, J., Zhang, P., Dal Corso, J., Yang, M., Wignall, P. B., Greene, S. E., et al. (2021). Volcanically driven lacustrine ecosystem changes during the Carnian Pluvial Episode (Late Triassic). *Proc. Natl. Acad. Sci. U. S. A.* 118:e2109895118. doi: 10.1073/pnas.2109895118

Lu, J., Zhang, P., Yang, M., Shao, L., and Hilton, J. (2020). Continental records of organic carbon isotopic composition ($\delta^{13}C_{org}$), weathering, paleoclimate and wildfire linked to the End-Permian Mass Extinction. *Chem. Geol.* 558:119764. doi: 10.1016/j.chemgeo.2020.119764

Mader, N. K., Redfern, J., and El Ouataoui, M. (2017). Sedimentology of the Essaouira Basin (Meskala Field) in context of regional sediment distribution patterns during upper Triassic pluvial events. *J. African Earth Sci.* 130, 293–318. doi: 10.1016/j.jafrearsci.2017.02.012

Mancuso, A. C., Benavente, C. A., Irmis, R. B., and Mundil, R. (2020). Evidence for the Carnian Pluvial Episode in Gondwana: new multiproxy climate records and their bearing on early dinosaur diversification. *Gondwana Res.* 86, 104–125. doi: 10.1016/j.gr.2020.05.009

Marchetti, L., Forte, G., Kustatscher, E., DiMichele, W. A., Lucas, S. G., Roghi, G., et al. (2022). The Artinskian Warming Event: an Euramerican change in climate and the terrestrial biota during the early Permian. *Earth Sci. Rev.* 226:103922. doi: 10.1016/j.earscirev.2022.103922

Mazaheri-Johari, M., Gianolla, P., Mather, T. A., Frieling, J., Chu, D., and Dal Corso, J. (2021). Mercury deposition in Western Tethys during the Carnian Pluvial Episode (Late Triassic). *Sci. Rep.* 11:17339. doi: 10.1038/s41598-021-96890-8

Mazaheri-Johari, M., Roghi, G., Caggiati, M., Kustatscher, E., Ghasemi-Nejad, E., Zanchi, A., et al. (2022). Disentangling climate signal from tectonic forcing: the Triassic Aghdarband Basin (Turan Domain, Iran). *Palaeogeogr. Palaeoclimatol. Palaeoecol.* 586:110777. doi: 10.1016/j.palaeo.2021.110777

Miller, C. S., Peterse, F., da Silva, A. C., Baranyi, V., Reichart, G. J., and Kürschner, W. M. (2017). Astronomical age constraints and extinction mechanisms of the Late Triassic Carnian crisis. *Sci. Rep.* 7:2557. doi: 10.1038/s41598-017-02817-7

Mueller, S., Hounslow, M. W., and Kürschner, W. M. (2016a). Integrated stratigraphy and palaeoclimate history of the Carnian Pluvial event in the Boreal realm; new data from the Upper Triassic Kapp Toscana Group in Central Spitsbergen (Norway). *J. Geol. Soc. Lond.* 173, 186–202. doi: 10.1144/jgs2015-028

Mueller, S., Krystyn, L., and Kürschner, W. M. (2016b). Climate variability during the Carnian Pluvial Phase — A quantitative palynological study of the Carnian sedimentary succession at Lunz am See, Northern Calcareous Alps, Austria. *Palaeogeogr. Palaeoclimatol. Palaeoecol.* 441, 198–211. doi: 10.1016/j.palaeo.2015.06.008

Olsen, P. E. (1997). Stratigraphic record of the early mesozoic breakup of Pangea in the laurasia-gondwana rift system. *Annu. Rev. Earth Planet. Sci.* 25, 337–401. doi: 10.1146/annurev.earth.25.1.337

Pecorari, M., Caggiati, M., Dal Corso, J., Cruciani, G., Tateo, F., Chu, D., et al. (2023). Weathering and sea level control on siliciclastic deposition during the Carnian Pluvial Episode (Southern Alps, Italy). *Palaeogeogr. Palaeoclimatol. Palaeoecol.* 617:111495. doi: 10.1016/j.palaeo.2023.111495

Peng, J., Slater, S. M., and Vajda, V. (2022). A Late Triassic vegetation record from the Huangshanjie Formation, Junggar Basin, China: possible evidence for the Carnian Pluvial Episode. *Geol. Soc. Spec. Publ.* 521, 95–108. doi: 10.1144/SP521-2021-151

Pott, C., Krings, M., and Kerp, H. (2008). The Carnian (Late Triassic) flora from Lunz in Lower Austria: paleoecological considerations. *Palaeoworld* 17, 172–182. doi: 10.1016/j.palwor.2008.03.001

Retallack, G. J., Veevers, J. J., and Morante, R. (1996). Global coal gap between Permian-Triassic extinction and Middle Triassic recovery of peat-forming. *Geol. Soc. Am. Bull.* 108, 195–207. doi: 10.1130/0016-7606(1996)108<0195:GCGBPT>2.3.CO;2

Rigo, M., Trotter, J. A., Preto, N., and Williams, I. S. (2012). Oxygen isotopic evidence for Late Triassic monsoonal upwelling in the northwestern Tethys. *Geology* 40, 515–518. doi: 10.1130/G32792.1

Roghi, G. (2004). Palynological investigations in the Carnian of the Cave del Predil area (Julian Alps, NE Italy). *Rev. Palaeobot. Palynol.* 132, 1–35. doi: 10.1016/j.revpalbo.2004.03.001

Roghi, G., Gianolla, P., Minarelli, L., Pilati, C., and Preto, N. (2010). Palynological correlation of Carnian humid pulses throughout western Tethys. *Palaeogeogr. Palaeoclimatol. Palaeoecol.* 290, 89–106. doi: 10.1016/j.palaeo.2009.11.006

Shen, J., Yin, R., Zhang, S., Algeo, T. J., Bottjer, D. J., Yu, J., et al. (2022). Intensified continental chemical weathering and carbon-cycle perturbations linked to volcanism during the Triassic-Jurassic transition. *Nat. Commun.* 13:299. doi: 10.1038/s41467-022-27965-x

Shi, Z., Jin, X., Preto, N., Rigo, M., Du, Y., and Han, L. (2019). The carnian pluvial episode at ma'antang, jiangyou in upper yangtze block, southwestern China. *J. Geol. Soc. Lond.* 176, 197–207. doi: 10.1144/jgs2018-038

Shi, Z., Preto, N., Jiang, H., Krystyn, L., Zhang, Y., Ogg, J. G., et al. (2017). Demise of Late Triassic sponge mounds along the northwestern margin of the Yangtze Block, South China: related to the Carnian Pluvial Phase? *Palaeogeogr. Palaeoclimatol. Palaeoecol.* 474, 247–263. doi: 10.1016/j.palaeo.2016.10.031

Simms, M. J., and Ruffell, A. H. (1989). Synchroneity of climatic change and extinctions in the Late Triassic. *Geology* 17, 265–268. doi: 10.1130/0091-7613(1989)017<0265:SOCCAE>2.3.CO;2

Sun, Y. W., Li, X., Liu, Q. Y., Zhang, M. D., Li, P., Zhang, R., et al. (2020). In search of the inland Carnian Pluvial Event: Middle–Upper Triassic transition profile and U–Pb isotopic dating in the Yanchang Formation in Ordos Basin, China. *Geol. J.* 55, 4905–4919. doi: 10.1002/gj.3691

Sun, Y. D., Wignall, P. B., Joachimski, M. M., Bond, D. P. G., Grasby, S. E., Lai, X. L., et al. (2016). Climate warming, euxinia and carbon isotope perturbations during the Carnian (Triassic) Crisis in South China. *Earth Planet. Sci. Lett.* 444, 88–100. doi: 10.1016/j.epsl.2016.03.037

Tomimatsu, Y., Nozaki, T., Sato, H., Takaya, Y., Kimura, J. I., Chang, Q., et al. (2021). Marine osmium isotope record during the Carnian "pluvial episode" (Late Triassic) in the pelagic Panthalassa Ocean. *Glob. Planet. Change* 197:103387. doi: 10.1016/j.gloplacha.2020.103387

Trotter, J. A., Williams, I. S., Nicora, A., Mazza, M., and Rigo, M. (2015). Long-term cycles of Triassic climate change: a new $\delta^{18}O$ record from conodont apatite. *Earth Planet. Sci. Lett.* 415, 165–174. doi: 10.1016/j.epsl.2015.01.038

Zhang, Y., Li, M., Ogg, J. G., Montgomery, P., Huang, C., Chen, Z. Q., et al. (2015). Cycle-calibrated magnetostratigraphy of middle Carnian from South China: implications for Late Triassic time scale and termination of the Yangtze platform. *Palaeogeogr. Palaeoclimatol. Palaeoecol.* 436, 135–166. doi: 10.1016/j.palaeo.2015.05.033

Zhang, P., Lu, J., Yang, M., Bond, D. P. G., Greene, S. E., Liu, L., et al. (2022b). Volcanically-induced environmental and floral changes across the Triassic-Jurassic (T-J) transition. *Front. Ecol. Evol.* 10:853404. doi: 10.3389/fevo.2022.853404

Zhang, P., Yang, M., Lu, J., Bond, D. P. G., Zhou, K., Xu, X., et al. (2023a). End-Permian terrestrial ecosystem collapse in North China: evidence from palynology and geochemistry. *Glob. Planet. Change* 222:104070. doi: 10.1016/j.gloplacha.2023.104070

Zhang, P., Yang, M., Lu, J., Jiang, Z., Zhou, K., Liu, H., et al. (2023b). Middle Jurassic terrestrial environmental and floral changes linked to volcanism: evidence from the Qinghai-Tibet Plateau, China. *Glob. Planet. Change* 223:104094. doi: 10.1016/j.gloplacha.2023.104094

Zhang, P., Yang, M., Lu, J., Shao, L., Wang, Z., and Hilton, J. (2022a). Low-latitude climate change linked to high-latitude glaciation during the late Paleozoic ice age: evidence from terrigenous detrital kaolinite. *Front. Earth Sci.* 10:956861. doi: 10.3389/feart.2022.956861

Zhao, H., Grasby, S. E., Wang, X., Zhang, L., Liu, Y., Chen, Z. Q., et al. (2022). Mercury enrichments during the Carnian Pluvial Event (Late Triassic) in South China. *GSA Bull.* 134, 2709–2720. doi: 10.1130/B36205.1

Zhou, T., and Zhou, H. (1983). Triassic non-marine strata and flora of China. *Bull. Chinese Acad. Geol. Sci.* 5, 95–110.